

SOLAR-WIND INDUCTION AND LUNAR CONDUCTIVITY

C.P. SONETT

*Department of Planetary Sciences, Lunar and Planetary Laboratory,
University of Arizona, Tucson, Ariz. (U.S.A.)*

(Accepted for publication February 27, 1975)

A summary review of electromagnetic induction driven in the Moon by the interplanetary magnetic field is given. The point of view developed centers on inversion of Fourier transforms of the magnetic field in the free-stream solar wind (forcing function) and the response on the lunar surface measured by Lunar Surface Magnetometers. Conductivity profiles are shown to depend upon the central angle between the magnetometer given by local time and the incident wave-normal direction. The induction excites at least magnetic dipole and quadrupole “radiation”, but any scattered field is confined to the Moon’s interior, save for propagation down the cavity where a TE-mode surface wave is generated. Confinement of the induced field on the sunward hemisphere and near the subsolar point is nearly complete, decreasing to the limbs, while in the diamagnetic cavity downstream of the Moon, partial confinement takes place. Both time and spatial multipoles of the induced field are present in the lunar interior complicating inversion into conductivity profiles. Profiles are reviewed and resolution limits are given and compared to those obtained from transient analysis. Finally a qualitative comparison to conductivity in the Earth is given.

1. Introduction

In its flow about the Moon the solar wind impacts directly upon the sunward surface; on the dark or antisolar hemisphere a cavity is formed from the target obscuration of the solar wind by the Moon itself (Colburn et al., 1967; Ness et al., 1967; Lyon et al., 1967). Pressure balance across the cavity requires that the interplanetary magnetic field be magnified therein, because of the decreased plasma pressure in the cavity. The solar wind is a diamagnetic fluid; the diamagnetism is manifested within the cavity as an increase of magnetic field. At the limbs of the Moon where the solar wind grazes the surface there is usually a large increase in magnetic field, sometimes accompanied by the occurrence of a weak shock wave (Siscoe et al., 1969; Sonett and Mihalov, 1972). These effects disappear when the Moon is shielded from the direct flow of the solar wind, i.e. when it is within the magnetic tail of the Earth. There, while restricted to the plasma sheet defining the separation of the two lobes of the tail, the presence of a disturbance field is noted (Schubert et al., 1974a). Even away from the sheet, but still within the tail where the plasma density

is least, true-vacuum conditions are still not approached. Electromagnetic effects are still present but free of the flow of streaming plasma (Smith et al., 1974).

The Moon is immersed in an electromagnetic field whose component fields are the interplanetary magnetic field and the motional electric field of the solar wind. The latter arises as a consequence of the relative motion of the solar wind and the Moon, and the high conductivity of the plasma; it can be expressed directly from the Lorentz invariance of the Maxwell equations. Though the electric field E transforms as $-\mathbf{V}_s \times \mathbf{B}$, where \mathbf{V}_s is the bulk speed of the solar wind with respect to the Moon, and \mathbf{B} is the interplanetary magnetic induction, \mathbf{B} transforms into itself nonrelativistically, which is always the case for the solar wind. Since $E = 0$ in the frame moving with the solar wind, it is apparent that the electric field seen by the Moon will be given by $-\mathbf{V}_s \times \mathbf{B}$.

Both components of the total electromagnetic field contain irregularities. The magnetic-field variations arise from convected tangential discontinuities (Burlaga, 1971) and diverse plasma waves (Belcher and Davis Jr., 1971) which propagate but are also convected at speeds far in excess of the propagation speed.

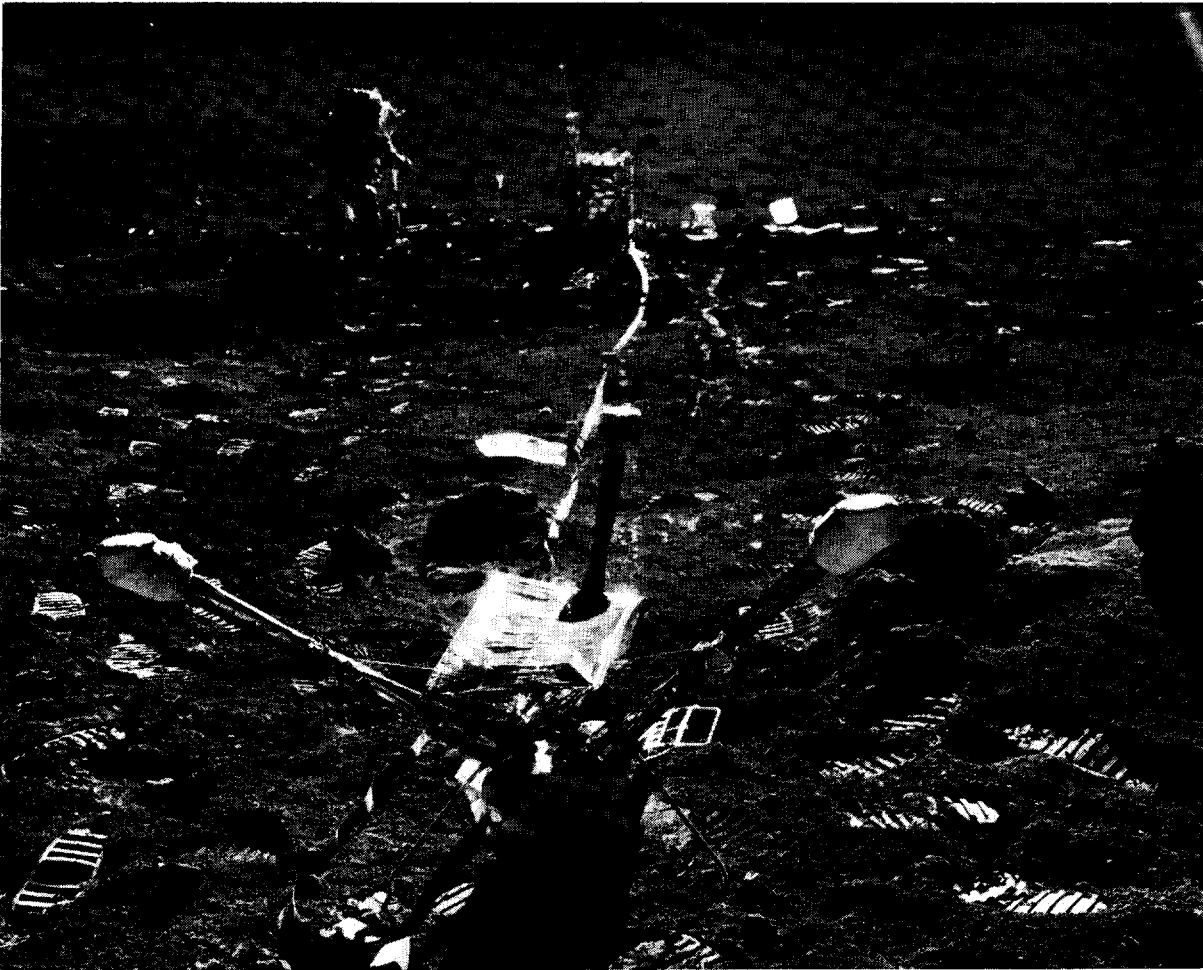


Fig. 1. Apollo-15 Lunar Surface Magnetometer (LSM) shown just subsequent to deployment at Hadley site just forward of the ALSEP central station (NASA photograph).

Both E and B are conceptually important in induction in a “bare” planet, i.e. one devoid of an insulating atmosphere or a magnetosphere and possibly in other cases.*

Induction by the interplanetary electric field corresponds to the transverse magnetic (TM) mode, while that due to the magnetic field corresponds to the transverse electric (TE) mode of classical electromagnetic theory (Schubert and Schwartz, 1969). Workers

* Planets can be classified as “bare”, having an atmosphere, a magnetosphere, or both. We have previously suggested (Sonett and Colburn, 1967, 1968) the terms geospheric, atmospheric and magnetospheric, leaning heavily upon terminology already a part of the vernacular.

in the field of global Earth induction will recognize the analogy. There, only the TE mode is excited because the insulating atmosphere inhibits the flow of vertical currents. In the case of the Moon, an “idealized” bare planet, the excitation by the electric field has not been detected. The low crustal conductivity of the Moon is hypothesized to inhibit direct electrical contact between the more conducting interior and the solar wind. If present, such contact would signify a total-path impedance sufficiently small that a steady-state electric current would be drawn between the solar wind and the lunar interior sufficient to cause the formation of a steady-state bow shock wave; it is the lack of such a wave, with the possible exception

of some vestigial effects at the limb, which leads to the conclusion that the TM mode is not significant (Sonett and Colburn, 1967, 1968). Although it might be assumed that the peak TM response could take place at non-zero frequency, this does not turn out to be the case and the above conclusion appears firm (Sonett and Colburn, 1974). The lack of a perceptible TM mode permits evaluation of the inductive signals in the Moon to be substantially simplified.

Fig. 1 shows the deployed ground station (ALSEP) for the Apollo-15 landing. This configuration at Hadley is nearly the same as for Apollo 12. The magnetometer (LSM) is shown in the foreground with the sun shade used to protect the central electronic container at the base. Immediately after the deployment of the Apollo-12 Lunar Surface Magnetometer (LSM) at the Oceanus Procellarum site, discovery of an inductive signal of spectacular amplitude in the Moon was made in response to a forcing field that consisted of a tangential discontinuity (Sonett et al., 1971). The signal transient amplitude of approximately 60γ seen at LSM takes place in the presence of an interplanetary field of relatively constant magnitude, $|B|$.

The vacuum response of a conducting sphere is at most $3/2$ that of the forcing field. For the sunward lunar hemisphere the solar wind plasma dynamic pressure, approximately 10^{-8} dyne/cm² during times of solar quiet, *forces the induced field back into the Moon*. That this could happen was surmised more than a decade ago by Neugebauer (1960), in attempting to explain the negative findings of Lunik II in its search for a permanent lunar field (Dolginov et al., 1961). Not only is the induced field confined to the lunar interior, but the high-frequency field must be confined to the crust. Otherwise the interior volume of confinement in the Moon would be large and the amplification only slightly larger than for a vacuum. From these comments and the frequency dependence of skin depth it follows that a steeply rising conductivity profile exists within the crust. When the solar wind is viewed as a fluid, the pressure normal to the surface should decrease away from the stagnation (subsolar) point and towards the limbs. Some imperfection in field confinement may take place near the limbs due to the reduced plasma pressure, a result substantiated at least partially by the excess fields often seen there (Coleman Jr. et al., 1972). Given a "quiet-time" solar wind dynamic pressure of 10^{-8}

dyne/cm², the equivalent field intensity is of the order 50γ . Since the induced field of Fig. 2 rises to this value or more, it is plausible that the confinement limit has been reached for this case. Although all of the details of the flow of a tangential discontinuity against the Moon have not been worked out in connection with the confinement, it is certain that a strong near-surface current layer exists in the solar-wind plasma upstream of the front hemisphere of the Moon. This current layer must come from the pressure gradients in the plasma; an important source of these is the confinement of the field.

2. Lunar transfer function

For purposes of analysis the electromagnetic response is defined by a strictly empirical procedure. Time-series recordings of magnetic field, both at LSM and Explorer-35 lunar satellite (required for determining the forcing function), are Fourier transformed into the frequency domain (Sonett et al., 1972). The transfer function, $A_i(f)$ is defined by:

$$h_{2i}(f) + h_{1i}(f) = A_i(f) \cdot h_{1i}(f) \quad (1)$$

where $[h_{2i}(f) + h_{1i}(f)]$ are the Fourier-transformed time series of the magnetic field components in ALSEP coordinates at ALSEP and Explorer 35 respectively. \hat{x} is the unit vector positive outwards and normal to the surface of the Moon at the ALSEP site, \hat{y} is positive easterly, and \hat{z} positive northerly, in the sense of customary compass headings. These ALSEP coordinated are basic to most of the following discussion. The parameter f is the frequency and $A_i(f)$ is a column vector; near the limbs, twisting of the field lines may introduce cross-coupling and makes $A(f)$ a tensor. The summed response shown on the left side of eq. 1 is the actual response measured on the surface. Separation of the forcing field from LSM data is not made using an angular distribution of stations as on Earth; Explorer 35 makes a direct measurement of this quantity. The induced field alone at the surface is given by:

$$[A_i(f) - 1] \cdot h_{1i}(f)$$

Fig. 2 shows the composite component transfer functions derived from more than one hundred hours of time swaths. The solid lines represent front or

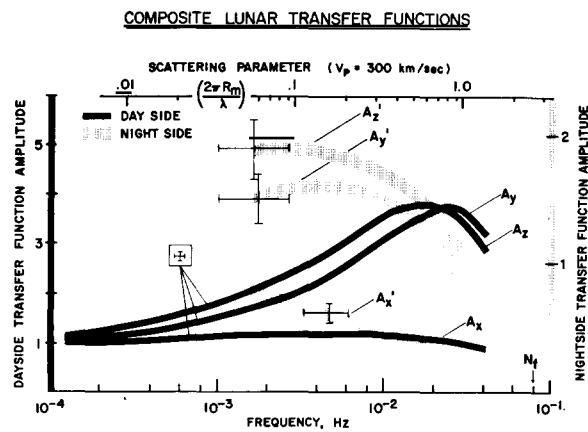
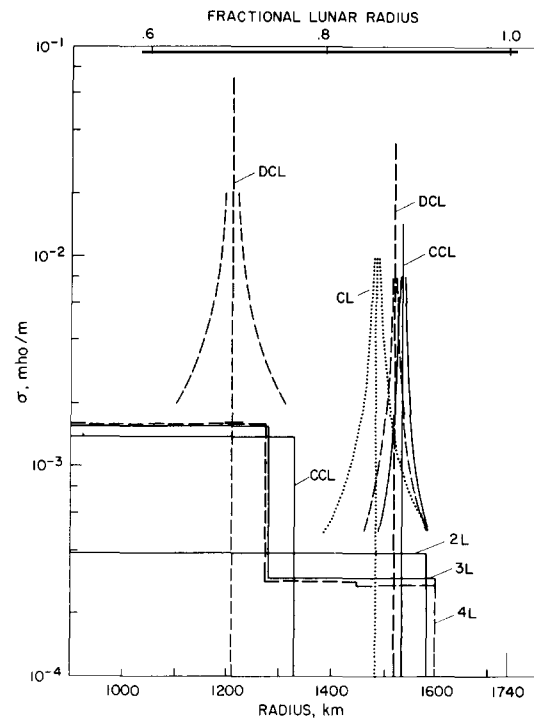


Fig. 2. Composite of component transfer functions including both dayside (solid) and darkside (shaded) data. Vertical range for the error bars is determined by the standard error; horizontal resolution is set approximately by $6/T$ where T is the swath length. The scattering parameter in the upper abscissa shows that at low frequency the Moon is a Rayleigh pseudoscatterer while for intermediate and high frequencies it corresponds to a Mie pseudoscatterer. The characteristic rollover at the high-frequency end of the spectrum is associated with mutual interference between the magnetic dipole and quadrupole.

sunward hemisphere data while the shaded lines refer to dark hemisphere data. The front-side data rises to a peak value of nearly $A_{y,z} = 4$ while on the dark side the amplitude of the two tangential components A_y and $A_z \lesssim 2$ but is still higher than the vacuum maximum of 1.5. The extended low-frequency data for the front side of the Moon is a result of having substantially longer time swaths than for dark data. The lesser mean-square-standard errors for the front (sunward hemisphere) are indicative of a much greater bank of data.

A_x is nearly unity over the whole frequency span confirming the use of a confinement of the scattered fields by a surface current layer in the theoretical analysis. However, the condition is not exact, as a slight rolloff exists at the high-frequency end of the transfer-function range. This is presently not understood; one hypothesis is that plasma waves are generated at sufficiently high frequency so as to propagate upstream, especially when away from the subsolar point where the normal component of the hypersonic stream velocity is reduced. If correct this would indicate that the boundary condition is "dispersive".

On the dark side of the Moon the behavior of A_x



— from Sonett, *et al.*, 1972

Fig. 3. Composite of current-layer (CL), double-current-layer (DCL), core-plus-current-layer (CCL), two-layer (2L), three-layer (3L), and four-layer (4L) models obtained from inversion of sunward data. The iteration is forced only to maintain model type; conductivity and radius are determined by calculation. Current layer models correspond qualitatively to the Backus-Gilbert resolution and "merge" into monotonic models as shown. These models are based upon a scattering angle $\theta = 150^\circ$ and $V_p = 200$ km/sec (Sonett *et al.*, 1972).

masquerades as a vacuum response. These data can be inverted into a conductivity profile using vacuum-scattering theory, but the result indicates a nearly constant conductivity Moon from the maximum resolution depth to the surface (Schubert *et al.*, 1973a). This is clearly inconsistent with other calculations as will be seen later.

One of the most distinctive features of the data of Fig. 2 is the rollover at high frequency for both the front and dark hemispheres. The rollover is attributable to mutual interference between the dipole and higher orders arising because of the cavity and because the wavelength of the driving field is comparable to the size of the Moon. In line with this the upper abscissa shows the scattering parameters $2\pi R_m/\lambda$

based upon a solar-wind wave phase velocity $V_p = 300$ km/sec.

Since the frequencies involved in lunar induction are extremely small, displacement currents can be ignored. The Moon is highly dissipative, and it is customary to use the decay time for eddy currents as a measure of the conductivity (Dyal and Parkin, 1971; Sill, 1972; Vanyan et al., 1973). This is appropriate for transient analysis, but the formalism used here and for Earth induction is cast fundamentally in terms of a wave equation albeit with highly damped propagation. The theory is formally identical to Mie scattering and at long-wavelength tends to the Rayleigh limit, save for the lack of a radiated scattered wave (Sonett and Colburn, 1974).

3. Theory

Lunar electromagnetic induction is complicated by the involved geometry, the plasma confinement on the sunward side and the cavity behind the Moon. Any attempt to understand the process as well as to invert data in the classical geophysical sense into a conductivity profile, may fail without adequate theory. Theoretical work has been under way since before the onset of the LSM experiment and has been aimed at solving the TE wave equation under difficult boundary conditions which are determined partially by the magnetohydrodynamic flow field surrounding the Moon. A full theory including high frequencies would involve "dispersive" boundary conditions, i.e. higher-frequency waves have sufficient characteristic speed in the solar-wind plasma to be able to escape confinement. But the energy density is likely insufficient to be of interest, and in any event, such frequencies lie far outside the passband of the magnetometers.

In spite of the formal similarity of the theory to Earth induction, loss of symmetry is entailed by the introduction of the cavity field. The higher-order modes of the lunar problem preclude any simple description of the forcing field (Schubert and Schwartz, 1969). These statements must be regarded in the light of some comparison standard. That is furnished by Schubert and Schwartz (1969), who employed spherically symmetric plasma (SSP) confinement. Forward calculations, using models developed from inversion with the SSP theory, permit

a definable standard to be given in terms of the mean-square residual standard error between a forward calculated transfer function and that representing the data (Sonett et al., 1972). The SSP theory assumes a spherical-symmetric Moon with radially continuously stratified conductivity. Although the formal identity of the SSP theory with Mie scattering has been explored (Sonett and Colburn, 1974), and the scattering parameter shown to characterize the relative strength of the magnetic multipoles excited, it is clear that total confinement of the induced field cannot permit a radiated wave. We employ the term pseudoscattering for the phenomenon where the wave associated with the induced field is entirely contained within the Moon.

The introduction of the cavity into the problem causes a perturbation having a scale comparable to that of the Moon. It is therefore not surprising that the solution under these conditions yields spatial multipoles of the field. The first version of this theory used a magnetic scalar potential within the Moon and the cavity, where currents are hypothesized to flow along the boundaries, restricting the scattered field (Schwartz and Schubert, 1973a). In this problem the lunar interior is characterized by two layers, the core being of infinite conductivity and the crust non-conducting. The limited symmetry of this problem means that the wave-normal direction must be known, though in the low-frequency limit the wavelength spectrum of the solar wind need not be specified. The pseudoscattering angle, θ , lies between the outward positive k vector and the position of LSM on the surface specified by the local lunar time. The solar-wind bulk speed, V_s and the phase velocity V_p will generally differ. The latter is defined along the direction of k , and its magnitude is V_s resolved in that direction.

Schubert et al. (1973b) have solved the more general case for higher frequency, but in both cases the problem is so far restricted to k parallel to the cavity axis. Schubert et al. show that a TE-mode wave propagates lengthwise in the cavity. A low-frequency cutoff of about 60 Hz is calculated; this is conceptually interesting and shows that some scattered radiation is present, but the frequencies are probably too high to be of general interest in the conductivity problem. Arbitrary k vector direction still remains an important problem for a full inversion of data.

A physically intuitive view of the effects of intro-

duction of the cavity into the induction problem is given by noting that lines of the induced field on the sunward side of the Moon are carried back into the cavity in complete analogy with the Earth's magnetosphere (Schubert et al., 1973c; Schwartz and Schubert, 1973b; Smith et al., 1973). The details seen in calculation (Schubert et al., 1973c) of the form of the induced magnetosphere show that even the dipole axis is tilted forward into the solar wind in analogy with that for Earth, but the comparison fails to include the null lines of the Earth's magnetosphere since reconnection is forbidden in nondeformable conductors.

4. Inversion and conductivity profiles using SSP theory

Conductivity profiles resulting from inversion of sunward hemisphere data taken from Sonett et al. (1972) are given in Fig. 3. A range of standard model types is included. Their suitability is tested by comparison of the square error residue between the forward calculated transfer function using these models and the actual data transfer functions.

The inversion is carried out by demanding an iterative fit to a specified case, e.g. three layer, *but the radius of each layer and its conductivity are freely determined in the iteration*. In addition, the phase velocity, V_p , and the pseudoscattering angle, θ , are chosen to cover a range of values approximating reasonable solar-wind conditions and the position of the LSM in local lunar time. For purposes to be made clear shortly, the model choice is divided into monotonic two layer (2L), three layer (3L), four layer (4L), and a group including current discontinuities, i.e. current layer (CL), double-current layer (DCL), and core-plus-current layer (CCL). Current layers are characterized by their radial position and conductivity-thickness product, $\sigma\delta$, an admittance given in units of mho. Conceptually these are qualitatively indicative of resolution.

A range of values of $V_p = 200, 300, \text{ and } 400 \text{ km/sec}$ is given in Sonett et al. (1972) together with $\theta = 120^\circ, 130^\circ, 150^\circ, \text{ and } 180^\circ$. There is little choice between the 3L and 4L models signifying a lack of resolution at this level of detail. Table I showing the average difference between the mean error of a specific model and the data transfer function taken over all choices of V_p and θ , indicates little difference between 3L, 4L,

TABLE I

Mean differences averaged over V_p and θ between models and data transfer function

| Model | Mean error |
|-------|------------|
| CL | 2.97 |
| 2L | 1.01 |
| 3L | 0.50 |
| 4L | 0.60 |
| CCL | 0.47 |
| DCL | 0.36 |

CCL and DCL, but CL and 2L models are emphatically ruled out. (The square internal error of the data summed over the pass band is $\epsilon^2 = 0.70$.) It is clear that the resolution deteriorates beyond usefulness in attempting to distinguish between the more complex models.

The reader is referred to Sonett et al. (1972) for a complete description of the calculations and their differences. The best fit is found for $V_p = 200 \text{ km/sec}$. But this is puzzling for the mean spiral angle of the interplanetary magnetic field is 45° ; thus V_p would be expected to be about 300 km/sec , if Alfvén waves propagating down the lines of force (Belcher and Davis Jr., 1971) are assumed to constitute the forcing field. It is quite possible that this simple assumption about the form of the forcing field is in error. The effects upon the conductivity profiles is not serious for the deep limit but raises difficulties if fine resolution near the surface is required. A_{\min} used in these calculations represents the minimum value for A and is found by making a compass rotation of the transfer function. This is required because of the anisotropy in A_y and A_z , which at the time of these calculations was thought to be associated with the permanent magnetic field at the Apollo-12 site. Similar results are found for conductivity profile changes with change in the pseudoscattering angle.

5. Darkside induction

This section discusses the induction problem when the LSM is in lunar night (Dyal and Parkin, 1971; Schubert et al., 1973a), and thus within the diamagnetic cavity. Fig. 4 gives theoretical transfer functions

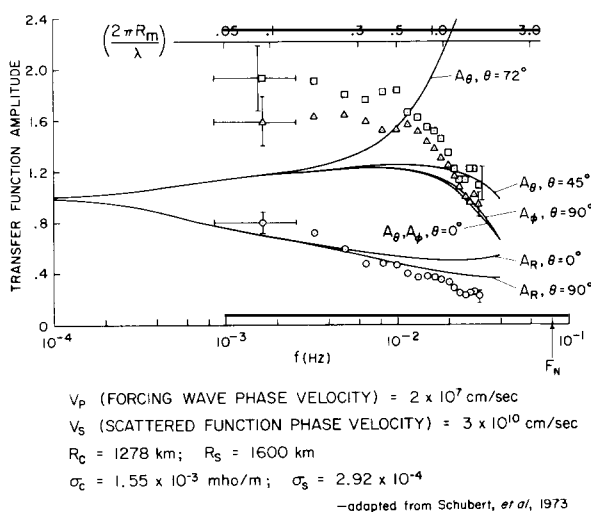


Fig. 4. Nightside lunar transfer functions with superimposed forward calculated transfer functions based upon the model of Fig. 3. The transfer functions shown correspond to varying θ , which has a profound effect upon the deviations from fit. The theory used for the forward calculations is quasi-vacuum. The forcing field phase velocity, $V_p = 200$ km/sec (adapted from Schubert et al., 1973c).

in a spherical polar set. A_r corresponds to A_x in the ALSEP set. For $\theta = 45^\circ$, the LSM is midway between the antisolar point (lunar midnight) and the limb of the Moon. In the great circle cross-section on the Moon containing the vector B , A_ϕ corresponds to the ALSEP \hat{z} (compass north) direction.

The transfer functions of Fig. 4 cover a more restricted range than for the sunward hemisphere because of the restricted time-swath lengths available. A forward calculation using the 3L model shown in Fig. 3 cannot be made to fit the data for any pseudo-scattering angle. The complications become even more extreme for the tangential functions, for it is apparent that no fit is attainable over the entire frequency range for any reasonably conceived values of θ and ϕ (Schubert et al., 1973a). The transfer functions used for these calculations are derived using a modified vacuum theory. That is, zero confinement is assumed but the forcing field $V_p = 200$ km/sec. On the basis that the plasma density in the cavity is very low, the wave speed there is assumed to be that of light in vacua. The purpose in this artifact calculation is to attempt to force a fit by the ruse of introducing higher-order time multipoles via the low phase speed. (Ordinary vacuum

theory intrinsically implies the speed of light and therefore fundamentally cannot supply the higher orders of the forcing field.)

A succinct summary of the theoretical aspects of the day–night differences and vacuum theory is given by Schubert et al. (1973b). That work shows tangential transfer functions for spherically symmetric vacuum (SSV) and asymmetric plasma confinement at midnight ($\theta = 0^\circ$), while the spherically symmetric plasma (SSP) and asymmetric-confinement results are compared at midday (local noon or the stagnation point of the solar wind with $\theta = 180^\circ$). The peak value of A for asymmetric confinement is reduced for $\theta = 180^\circ$ from the SSP value, indicating that some upward revision of the conductivity profile obtained there is required, provided that the assumption is made that the propagation is parallel to the cavity axis. That this is an oversimplification for the solar wind seems likely. For the dark side it is clear that differences also exist. But little more can be said except that these differences are due to the partial confinement and to the excitation of higher-order spatial harmonics of the field because of the presence of the cavity.

6. Signal anisotropy (polarization)

Recent results from Apollo 15 (Schubert et al., 1974b; Sonett et al., 1974) show that strong preferential (anisotropic) excitation takes place at this site. The effect begins to become apparent at about 5 mHz and dominates the response at high frequency. The implication of this polarized response is the presence of a local or regional conductivity anomaly in the Moon. A likely candidate supported by calculation is the Imbrium basin.

A similar but less prominent effect, noted in the early analysis of the Apollo-12 signals (Sonett et al., 1972), showed the direction of maximum response to be along the permanent magnetic field. This, together with the finding of a correlation between plasma dynamic pressure and the intensity of the local permanent field (Dyal et al., 1972), suggested that plasma-pressure fluctuations at the site contributed to the recorded induction in addition to that from the interior (Sonett et al., 1972). However, an adequate theory for this effect has not been developed. It was later determined that the anisotropy at Apollo 12

persisted into the cavity (during lunar night) when all effects of the incident solar wind should have been screened away. Thus the conditions producing the anisotropy at Apollo 12 remain enigmatic; perhaps it is associated with that producing the Apollo-15 response, but this is presently conjectural.

The effect upon determination of a conductivity profile remains to be assessed. The deep conductivity appears safe from major modification from this cause since the effect seems to vanish for very low frequency, but serious complication with the determination of the crustal conductivity may exist. This is analogous to Earth where, for deep sounding, spherical symmetry can be assumed (Banks, 1969), but for high frequencies the near-surface regions are known to require a more complex description than afforded by a symmetric theory (Rikitake, 1966).

7. The limit of deep sounding

Lunar induction has the distinguishing feature that the confinement intensifies the returned signal; this aids materially in raising the signal to noise ratio and is most apparent at the high-frequency end of the spectrum. As the frequency is lowered deeper penetration of the magnetic field takes place and the lunar volume excluding the field lines increases (Schwartz and Schubert, 1973b). Thus the determination of whether a conducting core is present depends upon low-frequency amplification which in turn becomes less important as the core depth is increased. The second significant effect with increasing depth of core is the geometrical inverse cube decrease in signal strength. Together these form the most significant constraints upon whether signal to noise ratio is sufficient for detection of a core of specified conductivity at a presumed depth. Schubert et al. (1973a) have examined this problem using computer simulations. They superimpose a core of conductivity 10^{-2} mho/m upon a Moon of constant conductivity $1.7 \cdot 10^{-4}$ mho/m. A core of radius $0.7 R_m$ is just detectable using the radial transfer function data for the darkside shown in this paper. The theoretical foundation for these calculations is quasi-vacuum theory, but there is no reason to suppose that more refined theory would lead to substantially different conclusions.

8. Comparison to Earth induction

In Fig. 5 we give a composite of several Earth models taken from reviews given at the last Edinburgh Workshop (Electromagnetic Induction in the Earth and Planets, 1973). The model of Banks (1969) shows a cutoff in resolution at depths less than about 0.1 Earth radius. The high-frequency limit for the data used was $2.9 \cdot 10^{-6}$ Hz. The lunar data shows conductivity profiles with greater internal consistency and values some four orders lower than for the Earth. The scaled crustal resolution is similar to that for the Earth, the near crust being inaccessible. The high-frequency limit for the lunar data is $4 \cdot 10^{-2}$ Hz. The lunar high-frequency limit is some $1.4 \cdot 10^4$ times that for the Earth. Conductivities for the two bodies differ widely, but an obvious scaling law using skin-depth arguments is apparent.

The lunar data shows the conductivity models discussed earlier and given in Fig. 3, while the shaded regions are estimates from transient response (Dyal and Parkin, 1971). The conductivity is shown to $0.3 R_m$, but based upon the discussion of Section 7, there appears no reason to assign a real significance to these estimates. Indeed both the Fourier transform and transient time domain responses fail to give significant resolution below about $0.7 R_m$, a condition expected to improve only by the analysis of more data, which would improve the statistics. A key difference between the time and frequency-domain models is the radius of the shell in the 3L model. The transient response results vary from 0.9 to $0.97 R_m$. Since these are based upon a vacuum model in the dipole limit, there appears no reason to place a high-confidence level upon them. On the other hand the addition of the anisotropy together with the generally incomplete account given by theory does not lend the utmost confidence to the results in general.

Although the Backus-Gilbert resolution criterion (Backus and Gilbert, 1967, 1968, 1970) has not been explicitly discussed in this paper, the spirit of it is contained in the combination of models for the frequency-response analysis. Unpublished resolution calculations do show a high consistency with the conclusions discussed here regarding the current layers and the general non-uniqueness of the models. The latter can be arrived at by noting the equivalent of the monotonic and non-monotonic spherical Moon

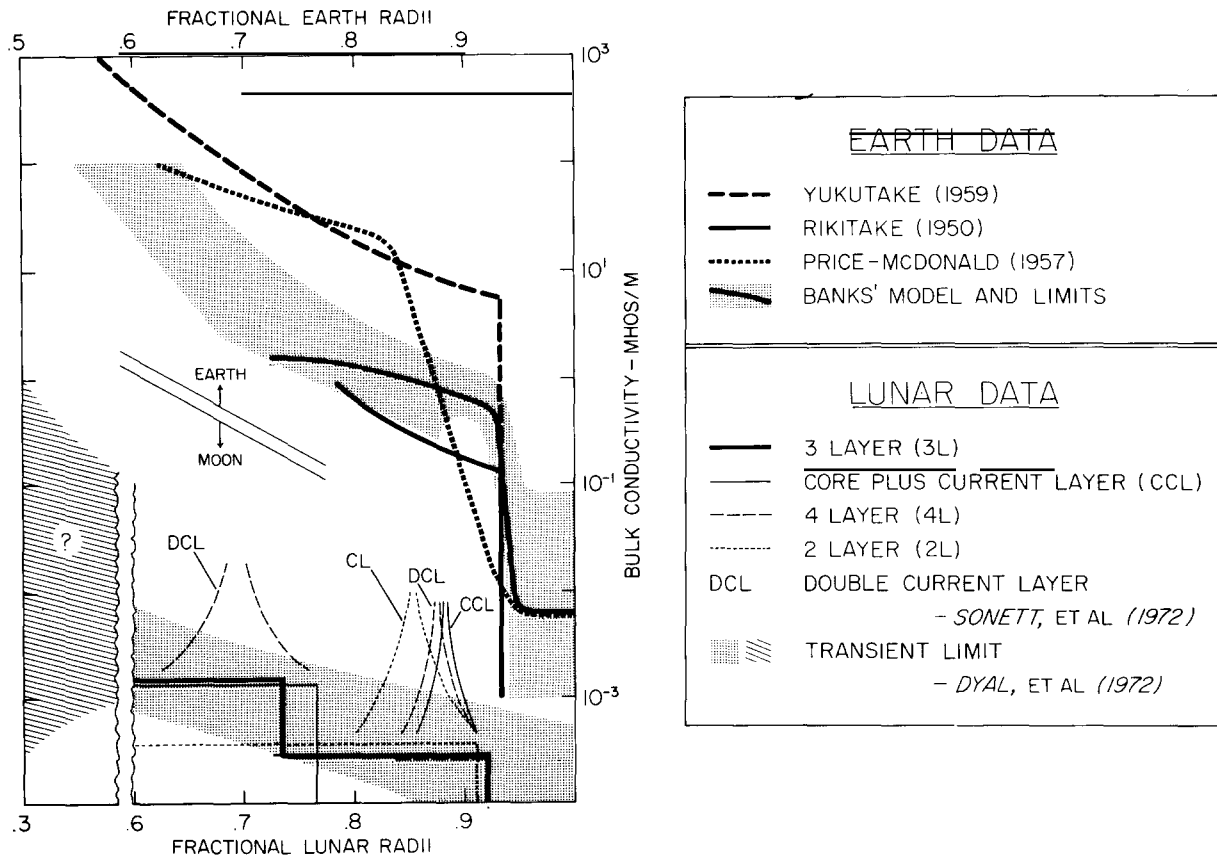


Fig. 5. Comparative conductivity profiles for the Earth and Moon using representative models for Earth and Moon. The shaded area in the lower figure is the range of transient models. The leftmost part is the deep transient estimate. Frequency-domain models are discussed in the text. The horizontal scale, similar for Earth and Moon is arranged for convenience. The vertical scale is identical for the two bodies. Both show a steep rise in crustal conductivity with depth, probably indicative of the effect of the thermal gradient upon conductivity.

models. The electrical response is quite similar for these models.

An important conceptual distinction may exist between the frequency and pulse analyses for the Moon; the former are based upon *restricted* heuristic inversions of transfer functions, while so far as this author is aware the pulse response uses a priori models. The difficulties of anisotropic induction are present equally for the two cases; a key difference is in the theory used for fitting. In the frequency-domain calculations, higher-order modes are admitted because the phase velocity can be taken into account. In the vacuum theory used for the transient analysis this is impossible except for the artifact of quasi-vacuum theory which, however has only been applied to the

frequency analysis. Differences due to confinement are given in detail in the text and not summarized here.

Measurement of lunar conductivity, begun some four years ago, now affords an internal view of the Moon competitive with that developed for the Earth. Because the lunar problem is still young and because the remaining path seems well established through our knowledge of the present limitations, there is hope that the conductivity profile for the Moon may be satisfactorily resolved to a depth greater than presently available. If the problems of the higher-order modes can be completed, then we should be able to resolve the crustal conductivity in a more satisfactory manner than the present data permit.

It is still likely, in the long view, that the conductivity profile may be more an indicator of the internal chemistry of the Moon than of the temperature. In any event it seems certain that the conductivity profile, by itself, can best give understanding of the internal thermal profile in association with other geophysical experiments.

For the standpoint of plasma physics the Moon, being a "bare" planet provides an unparalleled object for the study of the solar-wind interaction, a problem of equal importance for planets having an atmosphere or magnetosphere. I have deliberately not discussed the permanent magnetization of the Moon, a subject outside the scope of this paper. Nevertheless it should be said that the final untangling of lunar history will probably include this problem upon which the thermal evolution obviously has a profound bearing.

Acknowledgement

This work reports on my work jointly with my collaborators, G. Schubert, B.F. Smith, D.S. Colburn and K. Schwartz. I thank them for having read the manuscript, pointing out several errors. This work was supported under NASA grant NGS-7020.

References

- Backus, G.E. and Gilbert, J.F., 1967. *Geophys. J.R. Astron. Soc.*, 13: 247
- Backus, G.E. and Gilbert, J.F., 1968. *Geophys. J.R. Astron. Soc.*, 16: 169
- Backus, G.E. and Gilbert, J.F., 1970. *Philos. Trans. R. Soc. London, Ser. A*, 266: 123
- Banks, R.J., 1969. *Geophys. J.R. Astron. Soc.*, 17: 457
- Belcher, J.W. and Davis Jr., L., 1971. *J. Geophys. Res.*, 76: 3534
- Burlaga, L.F., 1971. *Space Sci. Rev.*, 12: 600
- Colburn, D.S., Currie, R.G., Mihalov, J.D. and Sonett, C.P., 1967. *Science*, 158: 1040
- Coleman Jr., P.J., Lichtenstein, B.R., Russell, C.T., Schubert, G. and Sharp, L.R., 1972. *Proc. 3rd Lunar Sci. Conf., Geochim. Cosmochim. Acta, Suppl. 3*, 3: 2271
- Dolginov, Sh.Sh., Yeroshenko, Ye.G., Zhuzgov, L.N. and Pushkov, N.V., 1961. *Geomagn., Aeron.*, 1: 18
- Dyal, P. and Parkin, C.W., 1971. *J. Geophys. Res.*, 76: 5947
- Dyal, P., Parkin, C.W., Snyder, C.W. and Clay, D.R., 1972. *Nature*, 236: 381
- Electromagnetic Induction in the Earth and Planets, 1973. *Proc. of the Workshop on Electromagnetic Induction, University of Edinburgh, September 20-27, 1972. Phys. Earth Planet. Inter.*, 7: 227
- Lyon, E.F., Bridge, H.S. and Binsack, J.H., 1967. *J. Geophys. Res.*, 72: 6113
- Ness, N.F., Behannon, K.W., Searce, C.S. and Cantarano, S.C., 1967. *J. Geophys. Res.*, 72: 5769
- Neugebauer, M., 1960. *Phys. Rev. Lett.*, 4: 6
- Rikitake, T., 1966. *Electromagnetism and the Earth's Interior. Elsevier, Amsterdam*, 308 pp.
- Schubert, G. and Schwartz, K., 1969. *Moon*, 1: 106
- Schubert, G., Smith, B.F., Sonett, C.P., Colburn, D.S. and Schwartz, K., 1973a. *J. Geophys. Res.*, 78: 3688
- Schubert, G., Schwartz, K., Sonett, C.P., Colburn, D.S. and Smith, B.F., 1973b. *Proc. 4th Lunar Sci. Conf., Geochim. Cosmochim. Acta, Suppl. 4*, 2909
- Schubert, G., Sonett, C.P., Schwartz, K. and Lee, H.J., 1973c. *J. Geophys. Res.*, 78: 2094
- Schubert, G., Lichtenstein, B.R., Russell, C.T., Coleman Jr., P.J., Smith, B.F., Colburn, D.S. and Sonett, C.P., 1974a. *Geophys. Res. Lett.*, 1: 97
- Schubert, G., Smith, B.F., Sonett, C.P., Colburn, D.S. and Schwartz, K., 1974b. *Science*, 183: 1195
- Schwartz, K. and Schubert, G., 1973a. *J. Geophys. Res.*, 78: 6496
- Schwartz, K. and Schubert, G., 1973b. *Moon*, 7: 279
- Sill, W.R., 1972. *Moon*, 4: 3
- Siscoe, G.L., Lyon, E.F., Binsack, J.H. and Bridge, H.S., 1969. *J. Geophys. Res.*, 74: 59
- Smith, B.F., Colburn, D.S., Schubert, G., Schwartz, K. and Sonett, C.P., 1973. *J. Geophys. Res.*, 78: 5437
- Smith, B.F., Colburn, D.S., Schubert, G., Sonett, C.P. and Schwartz, K., 1974. *EOS (Trans. Am. Geophys. Union)*, 55: 228
- Sonett, C.P. and Colburn, D.S., 1967. *Nature*, 216: 340
- Sonett, C.P. and Colburn, D.S., 1968. *Phys. Earth Planet. Inter.*, 1: 326
- Sonett, C.P. and Colburn, D.S., 1974. *Mie scattering of the interplanetary magnetic field by the whole Moon. In: T. Gehrels (Editor), Planets, Stars and Nebulae Studied with Photopolarimetry, University of Arizona Press, Tucson, Ariz.*, p. 419
- Sonett, C.P. and Mihalov, J.D., 1972. *J. Geophys. Res.*, 77: 588
- Sonett, C.P., Dyal P., Parkin, C.W., Colburn, D.S., Mihalov, J.D. and Smith, B.F., 1971. *Science*, 172: 256
- Sonett, C.P., Smith, B.F., Colburn, D.S., Schubert, G. and Schwartz, K., 1972. *Proc. 3rd Lunar Sci. Conf., Geochim. Cosmochim. Acta, Suppl. 3*, 3: 2309
- Sonett, C.P., Smith B.F., Schubert, G., Colburn, D.S. and Schwartz, K., 1974. *Proc. 5th Lunar Sci. Conf., Geochim. Cosmochim. Acta, Suppl. 5*, 3: 3073
- Vanyan, L.L., Berdichevsky, M.N., Yegorov, I.V. and Krass, M.S., 1973. *Ann. Géophys.*, 29, 3: 367